Intercontinental Geoinformation Days

igd.mersin.edu.tr

Checking Landsat 8 OLI's predictive power in the retrieval of chlorophyll-a and phycocyanin concentrations of a reservoir with high frequency field data

Güray Hatipoğlu[*1]

[1]*Middle East Technical University, Graduate School of Natural and Applied Sciences, Earth System Sciences, Ankara, Turkey*

Keywords
Remote sensing
water
chlorophyll-a
phycocyanin
landsat

ABSTRACT

Increased population, global warming, climate change, environmental pollution, agriculture, and many other issues make the monitoring of water bodies more and more critical with each day. Among the water quality variables to monitor, chlorophyll-a and phycocyanin are very crucial, as the former is strongly related to the phytoplankton dynamics, and the latter is an indicator of blue-green algae or cyanobacteria. As field trips are tiresome and difficult, satellite remote sensing methods have been developed continuously, yet most of the time their validation was insufficient since the aforementioned water quality variables may change dramatically with time. Hence, this study checked many commonly used algorithms reported to work well for chlorophyll-a retrieval with Landsat 8 OLI and an autosampler data which measures chlorophyll-a and phycocyanin in every 10 minutes. If not for the chlorophyll-a yet, a few band ratio algorithms and B1 and B6 of Landsat 8 OLI produced really promising prediction accuracies.

1. INTRODUCTION

The general issue in the remote sensing retrieval of chlorophyll-a (chla) is that global algorithms perform poorly on many different water bodies.

Tavares et al. (2021) constructed regionalized algorithms and reported superior performance over global ones, the best one was 2 band semi-analytical algorithm with red and near-infrared (NIR) bands of Sentinel-2 Multispectral Imager (MSI). Cui et al. (2020) too, considered regionally tuning the general algorithms after obtaining optical water type (OWT) and selecting an algorithm working best in that OWT for Bohai Sea. Still, OC4 algorithm of O'Reilly et al. (1998) was relatively successful even before regionalization. Matsushita et al. (2012) and Matsushita et al (2015) also made a similar approach, with having Case I and II differentiation in the former, and Maximum Chlorophyll Index (MCI) assigned category in the latter. Son and Kim (2018) also regionalized an algorithm after showing that OC4 was not good for their very low chla containing waters and generated a power function utilizing 4 bands in the blue-green region. Similar regionalization is applied by Al Shehhi et al. (2017) to account for the turbid atmosphere (i.e. dusty) of Arabia, and a power fit was obtained.

Moreover, there were uncountable study that developing/tuning new band algorithms, a few examples are Zhao et al. (2015), Huang et al. (2014), and Zhou et al. (2014). Among them, for instance, Rodríguez-López et al. (2020) checked many simple indices for Lake Laja chla retrieval, where chla concentrations were quite low, and found that combined use of normalized difference vegetation index (NDVI) and Green normalized difference vegetation index (GNDVI) yields very high correlation coefficient. For phycocyanin, Isenstein et al. (2020) used Landsat 7 ETM+ models for many groups of phytoplankton, and a model with R^2 of 0.83 was constructed against the square root of cyanobacteria volume in unit water volume.

One very common shortcoming of algorithm testing studies similar to above is the time difference between *in situ* sampling and satellite overpass. Chla, for instance, can vary in the order of minutes, but many studies worked with even a 2-day time difference. This study employs one dataset from Beaverdam Reservoir, Virginia, US with chla, phycocyanin, which are quite

* **Corresponding Author**

*(gurayhatipoglu@gmail.com) ORCID ID 0000 – 0002 – 7538 – 6265

Cite this study

Hatipoğlu G, (2021). Checking Landsat 8 OLI's predictive power for chlorophyll-a and phycocyanin concentrations of a reservoir with high frequency field data.. 2nd Intercontinental Geoinformation Days (IGD), 116-119, Mersin, Turkey

important for aquatic environments monitoring in 10-minute interval measurements. Owing to the relative smallness of the reservoir, it is impossible to retrieve anything with MODIS or Sentinel-3 satellites, but Landsat-8 OLI has sufficient spatial resolution. Landsat 8 OLI's bands and band ratio algorithms' predictive power for these variables are tested with almost simultaneous satellite match-ups to *in situ* data in this study.

2. METHOD

This section presents information about the study area, used *in situ* and satellite remote sensing data and the methods of the study.

2.1. Study Area

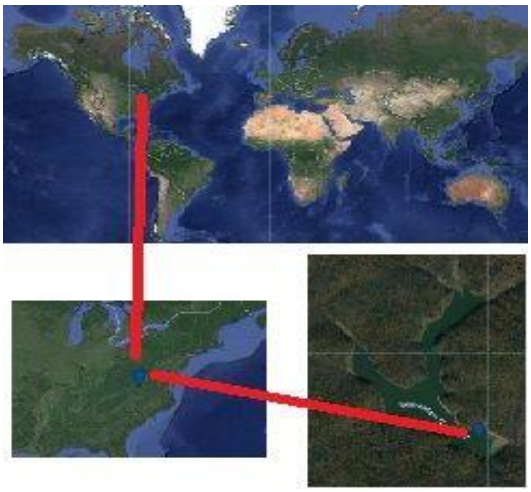

Figure 1. Location of the Beaverdam Reservoir (Google, n.d.)

Beaverdam Reservoir is situated roughly between 37.31 and 37.32 North latitudes, and -79.81 to -79.82 east longitudes. It is a secondary drinking water source for Roanoke, Virginia.

2.2. *in situ* Data

The part of the data matching up with the Landsat-8 OLI cloudless overpass was obtained from Carey et al. (2021). They collected *in situ* data via autosamplers that measure the water every 10 minutes. The chla, phycocyanin measurements were obtained via YSI EXO2 sonde. The mean, standard deviation, and range of these variables are in Table 1.

Table 1. Summary statistics of chlorophyll-a (chla) and phycocyanin (bga) data used in this study

Items	Mean	Standard Deviation	Range
chla(µg/L)	5.51	3.29	11.46
bga(µg/L)	0.27	0.16	0.49

2.3. Remote Sensing Data

Landsat 8 Operational Land Imager (OLI) top-of-atmosphere (TOA) reflectance (Chander et al. 2009) data were obtained via Google Earth Engine (Gorelick et al. 2017). (The atmospherically corrected data was not included in this study, as atmospheric correction itself heavily influences chla retrievals, and there might be algorithms that can still function well with TOA remote sensing data). 9 images of Landsat 8 OLI without clouds or other interferences were found within the period of *in situ* data presence. All images had Visible to NIR and short-wave infrared (SWIR) bands; B1,2,3,4 for coastal, blue, green, and red, respectively, then B5 as NIR, B6, and B7 as SWIR, B8 for the panchromatic band, B9 for cirrus detection, B10, and B11 for thermal bands (not used here). For the matched pixels, the correlogram between these bands is in Fig. 2.

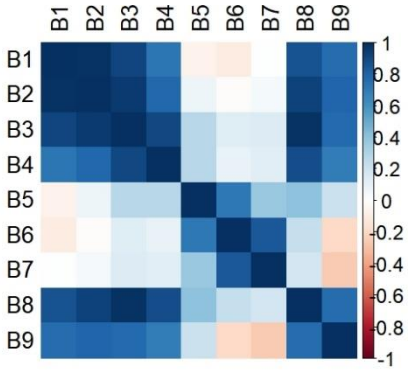

Figure 2. Correlogram of Landsat 8 OLI bands in this study's dataset

2.4. Methods

To check whether commonly applied band-ratio or other similar algorithms hold for high-frequency data match-ups as well, 10 widely used chla retrieval algorithms were chosen and presented in Table 2. (some of them mostly used for terrestrial purposes, but still retrieved chla).

Table 2. The indices used in retrieving chlorophyll-a (chla), and phycocyanin

Index	Structure	Reference
NDVI	(N-R)/(N+R)	(Rouse et al. 1973)
GNDVI	(N-G)/(N+G)	(Gitelson et al. 1996)
ARVI	(N-(R-(R-B)))/(N+(R-(R-B)))	(Kaufman & Tanre, 1992)
VARI	(G-R)/(G+R-B)	(Cheng et l. 2013)
VI Green	(G-R)/(G+R)	(Cheng et l. 2013)
GCI	(N/G)-1	(Gitelson et al. 2006)
NAVI	1-(Red/NIR)	(Carmona et al. 2015)
GDVI	NIR - Green	(Sripada et al. 2006)
EVI	2.5*((N-R)/(N+(6*R)-(7.5*B)+1)	(Huete et al. 2002)
NRVI	((R/N)-1)/((R/N)+1)	(Baret & Guyot, 1991)

Note: R stands for Red, G stands for Green, B stands for Blue, N stands for Near Infrared.
Note: ARVI index is used with coefficient of (R-B) as 1

The indices' performances were evaluated via R^2 adjusted values and Residual Standard Errors of the fitted linear models. As the dataset is very small yet, no training/test separation was done. All operations were done in R statistical environment (R Core Team, 2020).

3. RESULTS

Attempts to predict chla by indices failed. The following Table 3 shows relatively successful phycocyanin predictions.

Table 3. Performances of algorithms in retrieving phycocyanin concentration

Index	Adj R2 / RE for bga*
NDVI	(-)** 0.6081 / 0.1007
GNDVI	(-) 0.5564 / 0.1071
ARVI	(-) 0.5126 / 0.1123
VARI	(-) -0.09475 / 0.1683
VI Green	(-) -0.06856 / 0.1663
GCI	(-) 0.5 / 0.1137
NAVI	(-) 0.6301 / 0.09783
GDVI	(-) 0.4877 / 0.1151
EVI	(-) 0.5446 / 0.1085
NRVI	0.6081 / 0.1007

Note: *Adj R^2 stands for adjusted R^2, RE is residual standard error, bga is the phycocyanin concentration
Note: **(-) means that there is an inverse correlation

Table 4. Phycocyanin/chla ratio prediction performance

Index	Adj R^2 / RE for bgatochla*
NDVI	(-)** 0.3599 / 0.04354
GNDVI	(-) 0.3715 / 0.04314
ARVI	(-) 0.3122 / 0.04513
VARI	(-) -0.07602 / 0.05645
VI Green	-0.0718 / 0.05634
GCI	(-) 0.297 / 0.04563
NAVI	(-) 0.4405 / 0.0407
GDVI	(-) 0.606 / 0.03416
EVI	(-) 0.5324 / 0.03721
NRVI	0.3599 / 0.04354

Note: *Adj R^2 stands for adjusted R^2, RE is residual standard error, bgatochla is the ratio of phycocyanin to chla
Note: **(-) means that there is an inverse correlation

4. DISCUSSION

Even though chla was not successfully predicted in any algorithms, if one can modestly predict phycocyanin, and also the ratio of the phycocyanin to chla, it might be better than directly applying bands or indices to predict chla itself. Additionally, almost never used B1 coastal band predicts phycocyanin/chla with 0.5936 adjusted R^2 and 0.03469 residual standard error, and B6 shows similarly good performance of 0.5974 adjusted R^2 and 0.1021 residual standard error for phycocyanin retrieval itself (other bands' performances unreported, as they were very poor). Their linear model diagnostics, checking for any heteroscedasticity, very influential variables, were not bad, especially for the model with B6, albeit the good models for phycocyanin/chla ratio had influential one or two values. Additionally, as can be seen in Fig.2, B1 and B6 are only slightly and negatively correlated, so they are likely to carry different information. Hence, a new index to retrieve chla might be considered with either these B1 and B6 bands or NAVI and GDVI indices together with a much larger dataset.

5. CONCLUSION

Effective monitoring of the water bodies will be more and more widespread with more robust remote sensing retrieval of important water quality variables. This paper checked the predictive power of commonly used band-ratio algorithms, as well as the bands themselves, from Landsat 8 OLI to retrieve chla and phycocyanin concentrations from Beaverdam Reservoir in Virginia, US where there is a high-frequency sampler buoy that might be used to obtain satellite match-up with maximum 5 minutes of time lag.

Even though not for chla, there seem to be quite efficient ways to obtain phycocyanin, and also its ratio to chla via Landsat 8 OLI TOA reflectance. With an increased amount and availability of similar *in situ* data every day, algorithms including Band 1 and Band 6, or NAVI and GDVI indices should be developed for better retrieval of phycocyanin, which will make the monitor of cyanobacteria and its bloom much easier.

ACKNOWLEDGEMENT

The author is grateful to United States Geological Survey to distribute Landsat 8 OLI free for everyone, to Google Earth Engine team to allow everyone to access a wealth of remote sensing data very efficiently and with a cloud computing environment, to Cayelan C. Carey and her research team for making their data available in Environmental Data Initiative Repository with sufficient intellectual right access to use them after proper citation.

REFERENCES

Al Shehhi, M. R., Gherboudj, I., Zhao, J., & Ghedira, H. (2017). Improved atmospheric correction and chlorophyll-a remote sensing models for turbid waters in a dusty environment. *ISPRS Journal of Photogrammetry and Remote Sensing*, *133*, 46–60. https://doi.org/https://doi.org/10.1016/j.isprsjprs.2017.09.011

Carey, C.C., A. Breef-Pilz, and B.J. Bookout. (2021). Time series of high-frequency sensor data measuring water temperature, dissolved oxygen, pressure, conductivity, specific conductance, total dissolved solids, chlorophyll a, phycocyanin, and fluorescent dissolved organic matter at discrete depths in Beaverdam Reservoir, Virginia, USA in 2020 ver 1. Environmental Data Initiative. Retrieved in March 13, 2021 from: https://doi.org/10.6073/pasta/9a4877016583357cf04b8f68eb53b648.

Chander, G., Markham, B. L., & Helder, D. L. (2009). Summary of current radiometric calibration coefficients for Landsat MSS, TM, ETM+, and EO-1 ALI sensors. *Remote Sensing of Environment*, *113*(5), 893–903. https://doi.org/https://doi.org/10.1016/j.rse.2009.01.007

Cui, T. W., Zhang, J., Wang, K., Wei, J. W., Mu, B., Ma, Y., … Chen, X. Y. (2020). Remote sensing of chlorophyll a concentration in turbid coastal waters based on a global optical water classification system. *ISPRS Journal of Photogrammetry and Remote Sensing*, *163*, 187–201. https://doi.org/https://doi.org/10.1016/j.isprsjprs.2020.02.017

Gitelson, A. A., Kaufman, Y. J., & Merzlyak, M. N. (1996). Use of a green channel in remote sensing of global vegetation from EOS-MODIS. *Remote sensing of Environment*, *58*(3), 289-298.

Gitelson, A. A., Keydan, G. P., & Merzlyak, M. N. (2006). Three-band model for noninvasive estimation of chlorophyll, carotenoids, and anthocyanin contents in higher plant leaves. *Geophysical research letters*, *33*(11).

Google. (n.d.). Beaverdam Reservoir, Virginia. Retrieved March 14, 2021, from https://goo.gl/maps/tr5vKWwASiJeapAV9

Gorelick, N., Hancher, M., Dixon, M., Ilyushchenko, S., Thau, D., & Moore, R. (2017). Google Earth Engine: Planetary-scale geospatial analysis for everyone. *Remote Sensing of Environment*, *202*, 18–27. https://doi.org/https://doi.org/10.1016/j.rse.2017.06.031

Huang, C., Zou, J., Li, Y., Yang, H., Shi, K., Li, J., … Zheng, F. (2014). Assessment of NIR-red algorithms for observation of chlorophyll-a in highly turbid inland waters in China. *ISPRS Journal of Photogrammetry and Remote Sensing*, *93*, 29–39. https://doi.org/https://doi.org/10.1016/j.isprsjprs.2014.03.012

Huete, A., Didan, K., Miura, T., Rodriguez, E. P., Gao, X., & Ferreira, L. G. (2002). Overview of the radiometric and biophysical performance of the MODIS vegetation indices. *Remote sensing of environment*, *83*(1-2), 195-213.

Isenstein, E. M., Kim, D., & Park, M.-H. (2020). Modeling for multi-temporal cyanobacterial bloom dominance and distributions using landsat imagery. *Ecological Informatics*, *59*, 101119. https://doi.org/https://doi.org/10.1016/j.ecoinf.2020.101119

Kaufman, Y. J., & Tanre, D. (1992). Atmospherically resistant vegetation index (ARVI) for EOS-MODIS. *IEEE transactions on Geoscience and Remote Sensing*, *30*(2), 261-270.

Matsushita, B., Yang, W., Chang, P., Yang, F., & Fukushima, T. (2012). A simple method for distinguishing global Case-1 and Case-2 waters using SeaWiFS measurements. *ISPRS Journal of Photogrammetry and Remote Sensing*, *69*, 74–87. https://doi.org/https://doi.org/10.1016/j.isprsjprs.2012.02.008

Matsushita, B., Yang, W., Yu, G., Oyama, Y., Yoshimura, K., & Fukushima, T. (2015). A hybrid algorithm for estimating the chlorophyll-a concentration across different trophic states in Asian inland waters. *ISPRS Journal of Photogrammetry and Remote Sensing*, *102*, 28–37. https://doi.org/https://doi.org/10.1016/j.isprsjprs.2014.12.022

O'Reilly, J. E., Maritorena, S., Mitchell, B. G., Siegel, D. A., Carder, K. L., Garver, S. A., … McClain, C. (1998). Ocean color chlorophyll algorithms for SeaWiFS. *Journal of Geophysical Research: Oceans*, *103*(C11), 24937–24953.

R Core Team (2020). **R**: A language and environment for statistical computing. **R** Foundation for Statistical Computing, Vienna, Austria.

Rodríguez-López, L., Duran-Llacer, I., González-Rodríguez, L., Abarca-del-Rio, R., Cárdenas, R., Parra, O., … Urrutia, R. (2020). Spectral analysis using LANDSAT images to monitor the chlorophyll-a concentration in Lake Laja in Chile. *Ecological Informatics*, *60*, 101183. https://doi.org/https://doi.org/10.1016/j.ecoinf.2020.101183

Rouse, J., Haas, R.H., Schell, J.A., & Deering, D. (1973). Monitoring vegetation systems in the great plains with ERTS. Third Earth Resources Technology Satellite-1 Symposium- Volume I: Technical Presentations. NASA SP-351

Son, Y.-S., & Kim, H. (2018). Empirical ocean color algorithms and bio-optical properties of the western coastal waters of Svalbard, Arctic. *ISPRS Journal of Photogrammetry and Remote Sensing*, *139*, 272–283. https://doi.org/https://doi.org/10.1016/j.isprsjprs.2018.03.024

Sripada, R. P., Heiniger, R. W., White, J. G., & Meijer, A. D. (2006). Aerial color infrared photography for determining early in-season nitrogen requirements in corn. *Agronomy Journal*, *98*(4), 968-977.

Tavares, M. H., Lins, R. C., Harmel, T., Fragoso Jr., C. R., Martínez, J.-M., & Motta-Marques, D. (2021). Atmospheric and sunglint correction for retrieving chlorophyll-a in a productive tropical estuarine-lagoon system using Sentinel-2 MSI imagery. *ISPRS Journal of Photogrammetry and Remote Sensing*, *174*, 215–236. https://doi.org/https://doi.org/10.1016/j.isprsjprs.2021.01.021

Zhao, J., Temimi, M., & Ghedira, H. (2015). Characterization of harmful algal blooms (HABs) in the Arabian Gulf and the Sea of Oman using MERIS fluorescence data. *ISPRS Journal of Photogrammetry and Remote Sensing*, *101*, 125–136. https://doi.org/https://doi.org/10.1016/j.isprsjprs.2014.12.010

Zhou, L., Roberts, D. A., Ma, W., Zhang, H., & Tang, L. (2014). Estimation of higher chlorophylla concentrations using field spectral measurement and HJ-1A hyperspectral satellite data in Dianshan Lake, China. *ISPRS Journal of Photogrammetry and Remote Sensing*, *88*, 41–47. https://doi.org/https://doi.org/10.1016/j.isprsjprs.2013.11.016